A Surrogate-Based Approach for Bend-Twist Coupling Optimization of a Horizontal Axis Wind Turbine Composite Blade

Tiago F. G. Farias[1], Marco A. Luersen[1], Claudio T. da Silva[1]

[1]*Departament of Mechanical Engineering, Federal University of Technology - Paraná (UTFPR), Campus Curitiba*
Rua Deputado Heitor Alencar Furtado, 5000, 81280-340, Curitiba, Paraná, Brazil
tiagofarias@alunos.utfpr.edu.br, luersen@utfpr.edu.br, tavares@utfpr.edu.br

Abstract. A horizontal axis wind turbine blade is designed using the Blade Element Momentum Theory under the assumption of rigid body behavior. Then, a composite ply material is selected and a laminate is built to raise bend-twist coupling effects in the blade, analyzed by reciprocal fluid-structure interaction. The composite layup sequence is parametrized within Ansys Composites PrepPost from a Design of Experiments using Latin Hypercube Sampling, accounting for different laminations for the upper and lower blade skins, given both geometry and stress distributions differ for each surface. Obtained responses are then used to model a surrogate through artificial neural networks, which is then optimized using genetic algorithms, seeking maximizing the power output. The optimized layup improves the generator for 8.3% extra power when compared to a span wise unidirectional composite (i.e., zero-degree layup). The maximum axial displacement stands below a threshold of 3% span length, allowing it to sustain operation in overload conditions and simultaneously avoid tower collapse by blade strike.

Keywords: horizontal axis wind turbine (HAWT), aeroelasticity, composite tailoring, surrogate modeling, optimization.

1 Introduction

Low-power generators (micro or mini generators) typically have fixed pitch angles, restricting the range of wind speeds in which they present good performance. On the other side, active pitch control systems enable a broader range of operation, but are typically installed in high-power generators (at a gigawatts production scale), due to its complexity and implementation/maintenance costs. By employing passive pitch angle control mechanisms, it is possible to increase the range of operating speeds of a generator without sacrificing simplicity. This renders an opportunity of further disseminating this renewable energy source, especially in previously unfavorable or unviable circumstances. For reference and categorization purposes, in Brazil the ANEEL [1] defines the power limit for mini and micro generation as up to 5 MW (or 3 MW for hydro sources).

A study carried out by Hussni [2] shows the potential for wind power generation in large urban centers such as the city of São Paulo, Brazil, prospecting the installation of wind turbines on the tops of buildings. Hussni [2] also states that a major difficulty in disseminating this energy solution is because much of the technology is still acquired from imports, few suppliers are situated in national territory, and many do not have the necessary power curves for evaluation prior to installation or simply do not supply turbines that match the Brazilian wind map.

Wind turbines are classified according to the rotor shaft orientation and its operation mode: vertical or horizontal axis; with or without speed control. Horizontal axis wind turbines (HAWT) have greater efficiency in extracting the wind intrinsic energy, as well as access to stronger winds due to the possibility of building higher towers. On the other hand, vertical axis wind turbines (VAWT) can operate independently of the wind direction, with the disadvantage of having lower efficiency and greater fluctuations of forces in the structure, which can also raise harmonic problems, as already stated by Soriano and Rubio [3].

The main goal of this study is to optimize the lamination sequence of an unidirectional laminated composite blade, tailoring the bend-twist coupling behavior of the composite to maximize power generation, especially in overloaded conditions. A few constraints are added to account for physical or operational limitations. It is aimed to reach significant twisting of the blade, enough to relief aerodynamic loads without exceeding an upper limit for maximum axial displacement, reducing the turbine's actuator disc coning effect and avoiding tower collapse. The passive pitch angle control yields greater power for the generator and allows for operation in overloaded conditions, when the turbine would usually be shut down for safety or operational reasons (e.g., blade stalling).

In this work, attention is directed towards horizontal axis wind turbines without speed control (HAWT/VSWT) for microgeneration. Similar studies have been conducted, optimizing HAWT composite blades for their structural performance or aerodynamic responses, such as Monte, Castelli and Benini [4], Mitra and Chakraborty [5], or Zhang *et al* [6]. Therefore, most of them focuses on offshore or megawatt scale generation, employing more complex systems for turbine control, and few yet focuses on simpler turbine blades, applicable to microgeneration such as top of building in large urban centers.

2 Theoretical background

2.1 Blade Element Momentum Theory (BEMT)

The Blade Element Momentum Theory (BEMT) is the amalgam of the Blade Element Theory (BET) and the Momentum Theory (MT). Many authors [7] [8] [9] [10] [11] describe this theory, which combines the characteristics of the flow field and the aerodynamic properties of the rotor blades into singular functions that provide the resulting forces and, ultimately, the efficiency of the evaluated turbine.

MT accounts for the wake of turbulence expansion and rotation downstream the generator, introducing limitations for the generator's power coefficient according to its axial and tangential induction factors. As for BET, it provides a simplified way of analyzing the aerodynamic phenomena that occur instantaneously in the interaction of the fluidic flow with the generator blade as a function of the location in its span. BET takes as a fundamental hypothesis the idea that each annular section does not interact with the adjacent ones, which is acceptable for small variations in the axial induction factor of the velocity along the blade.

The basic hypothesis of BEMT is that any stresses caused to the generator blades are due to the change in the moment of air flow that crosses the annular differential area of the actuating disc, swept by the blade element. The hypothesis of radial independence between adjacent rings is also considered acceptable, although the axial induction factor is rarely uniform. By combining the BET equations with the conservation of linear and angular momentums, one can establish expressions for the axial and tangential induction factors of the blades according to the resulting forces from the triangle of velocities:

$$\frac{a}{1-a} = \frac{\sigma_r}{4\,sen\,\phi^2}\left[C_x - \frac{\sigma_r}{4\,sen^2\,\phi}C_y\right] \tag{1}$$

$$\frac{a}{1+a'} = \frac{\sigma_r C_y}{4\,sen\,\phi\,cos\,\phi} \tag{2}$$

where a and a' are the axial and tangential induction factors, respectively; ϕ is the tilt angle, defined as the sum of the blade twist and the airfoil angle of attack; σ_r is the chord solidity, and; C_x and C_y are simplified ways of representing the influence of lift and drag coefficients, as follows:

$$\sigma_r = \frac{Nc}{2\pi r} \tag{3}$$

$$C_x = C_D\,sen\,\phi + C_L\,cos\,\phi \tag{4}$$

$$C_y = C_L\,sen\,\phi - C_D\,cos\,\phi \tag{5}$$

where N is the number of blades, and c the airfoil chord length.

Studies conducted by Wilson and Lissaman [12] on the subject argue that the contributing portion of the drag coefficient is negligible and that it has little to no effect over the pressure drop through the actuating disc. Hence, eq. (1) and eq. (2) can be rewritten as:

$$a = \frac{\sigma_r C_L \cos\phi}{1+4\,sen^2\,\phi} \tag{6}$$

$$a' = \frac{1}{\frac{4\cos\phi}{\sigma_r C_L} - 1} \tag{7}$$

The error induced by the simplification of the drag coefficient becomes sufficiently small, or negligible, for blade tip velocity ratios greater than 3, as emphasized by Burton *et al* [8]. It should be noted, however, that the resulting equations have no analytical solution, and the drag and lift coefficients are obtained empirically or are approximated by computer simulation.

2.2 Classical Lamination Theory

The Classical Lamination Theory (CLT) accounts for some simplifications in order to estimate a laminated composite material's behavior and is extensively described by Reddy [13] and Kaw [14]. Basic hypothesis are:

1. Each ply presents elastic linearity and orthotropic behavior;
2. A plane stress state is assumed for the laminate ($\sigma_z = \tau_{xz} = \tau_{yz} = 0$);
3. The laminate deforms according to the Kirchhoff-Love assumptions of thin plates ($\gamma_{xz} = \gamma_{yz} = 0$);
4. The normal strain in the laminate thickness direction is negligible ($\varepsilon_z = 0$);
5. The layers of the laminate are perfectly bonded (no shear deformations, and zero thickness bonds).

The stress and strain distributions of a laminate, due to their possible variations in lamination sequences, can be different in each ply. Hence, even though maintaining linear behavior in each ply separately, the stresses are non-constant along the cross-section of the laminate. It is therefore necessary to obtain the equivalent stresses and strains for the entire laminate. The equivalent stresses are obtained from the transformed stiffness matrix and the laminate strains, which can be obtained from the ply material properties and its displacements.

Taking the theory's aforementioned assumptions and simplifications, the stiffness matrix of the laminate can be simplified by combining the mechanical properties of each ply and integrating it along its thickness. Then, the stresses can be formulated in one single expression, accounting for the configuration and composition of the laminate along with the applied forces and momentums, simplifying:

$$\begin{bmatrix} N_x \\ N_y \\ N_{xy} \\ M_x \\ M_y \\ M_{xy} \end{bmatrix} = \begin{bmatrix} A_{11} & A_{12} & A_{16} & B_{11} & B_{12} & B_{16} \\ A_{12} & A_{22} & A_{26} & B_{12} & B_{22} & B_{26} \\ A_{16} & A_{26} & A_{66} & B_{16} & B_{26} & B_{66} \\ B_{11} & B_{12} & B_{16} & D_{11} & D_{12} & D_{16} \\ B_{12} & B_{22} & B_{26} & D_{12} & D_{22} & D_{26} \\ B_{16} & B_{26} & B_{66} & D_{16} & D_{26} & D_{66} \end{bmatrix} \begin{bmatrix} \varepsilon_x^0 \\ \varepsilon_y^0 \\ \gamma_{xy}^0 \\ \kappa_x \\ \kappa_y \\ \kappa_{xy} \end{bmatrix} \tag{8}$$

Equation (8) expresses the laminate [ABD] stiffness matrix. The extensor stiffness matrix [A] relates the forces in the plane stress state to its strains; the deflector stiffness matrix [D], relates the moments to its curvatures, and; the coupling matrix [B], highlighted in gray, represents the coupling between forces and moments, or deformations and curvatures. Thus, it is possible to evaluate the coupling behavior of strains and curvatures caused in a laminate with linearly elastic orthotropic ply materials, once the applied forces are provided.

2.3 Artificial Neural Networks

The main concept of Artificial Neural Networks (ANN) is to construct a set of algorithms, modeled loosely after the human brain, designed to recognize patterns. Among others, radial based activation functions neurons are commonly used for ANN construction, also known as Radial Basis Functions (RBF).

As pointed by Ryberg, Bäckryd and Nilsson [15], RBFs refer to ANNs with radial based activation functions neurons. Each RBF has variables and parameters which builds the functions' behavior. Variables are those established in the Design of Experiments (DOE) (i.e., input dataset). Parameters are responsible for controlling the shape of the hypersurface (the model output), a n-dimensional mathematical representation of the evaluated system and learned data.

The Gaussian form is one of the most commonly used activation function in engineering problems for its high non-linearization response through simple weight variation (linearly). It can be represented as follows:

$$\psi(\gamma) = exp\left(-\gamma^2 \Big/ (2\sigma^2)\right), \gamma = \left(\sum_{j=1}^{k} \left| \boldsymbol{x}_j^{(i_1)} - \boldsymbol{x}_j^{(i_2)} \right|^p\right)^{1/p} \quad (9)$$

where $\psi(\gamma)$ is the activation function of pairwise sample distance γ; and σ is a parameter, used to model the functions' shape accordingly, this parameter can be declared as a scalar (constant value) or vector. When varying its value for each variable, it is a technique known as Kriging. As for the pairwise sample distance γ, it is computed from the difference of two samples $\boldsymbol{x}_j$ (using relative indexes i_1 and i_2) and norm p (usually Euclidian, $p = 2$).

As stated by Forrester, Sóbester and Keane [16], the model's calibration is paramount for performance, as it could either require too much computation to fit fast changing events (underfitting), or; wobble around the sampled points (overfitting), generating noise and decreasing the model's accuracy. Therefore, choosing the right parameter set or optimization techniques is key to good prediction capabilities, diminishing errors and narrowing confidence intervals, especially for non-linear interpolation. Optimization methods for tailoring the model are selected according to its characteristics and the dataset behavior, thus avoiding or diminishing under and overfitting.

2.4 Design optimization and evolutionary algorithms

Mathematically speaking, design optimization refers to maximizing (or minimizing) an objective function within certain constraints. In engineering, this translates to variables with associated characteristics from the studied system (e.g., to maximize power). An optimization problem can be formulated as:

$$\begin{aligned} \min_{\boldsymbol{x}} \quad & f(\boldsymbol{x}) \\ subject\ to \quad & g_i(\boldsymbol{x}) \leq 0 \\ & h_i(\boldsymbol{x}) = 0 \\ & x_{lower} \leq x_j \leq x_{upper} \end{aligned} \quad (10)$$

where $f(\mathbf{x})$ is the objective function evaluated at $\mathbf{x}$ (input dataset), subject to the corresponding restriction functions $g_i(\mathbf{x})$ and $h_i(\mathbf{x})$ within the acceptable variable interval $\{x_j \in [x_{lower}; x_{upper}] \subset \mathbf{x}\}$.

Among other authors, Arora [17] points that genetic algorithms are based on Darwin's theory of natural selection and belong to the class of stochastic search optimization methods. This method does not require continuity or differentiability of the cost function; however, it requires a large amount of calculations and relies heavily in random number generation, which may yield different solutions for different runs of the algorithm.

The method works with an initial population of designs (i.e., a subset, whose population size remains the same), and implements random processes seeking improvement of the average fitness of subsequent subsets. Some of the processes are: reproduction, crossover, mutation, and immigration. For the stopping criteria, it can be determined a maximum number of iterations or a threshold for the minimum improvement of the cost function after a defined number of consecutive iterations.

3 Methodology

In the present work, the layups of the upper and lower skins – high velocity, and high pressure surfaces, respectively – of a HAWT blade are optimized seeking maximizing the power generation, while limiting the maximum axial displacement. By doing this, it is expected to decrease the blade sections' angles of attack and relief aerodynamic loads, postponing stall and increasing torque. Figure 1 presents a summarized workflow of the employed methodology, as described in this section.

The blades' geometry is designed through an algorithm developed in Matlab by da Silva [18]. The algorithm implements Blade Element Momentum Theory (BEMT) to establish parameters such as blade twist, maximum span, chord lengths, etc. The blade geometry is defined with NACA 4412 airfoil profiles, except for the hub connection, where the blade profile is cylindrical. The blade's geometry is then remodeled in the QBlade software – which accounts for Prandt tip and root aerodynamic losses –, exported as STL format, and smoothed within Solidworks using an algorithm developed in Python and VBA by the author, compacting the geometry from 29957 facets to 122 smooth surfaces: tip closing; hub connection, and; 60 surfaces for the upper and lower skins of the blade, respectively.

Preliminary studies incorporate mesh sensitivity analysis (to increase computational efficiency), stiffness evaluation (stress and strains in normal conditions), and composite predefinition (number of plies and material).

DOE points are generated through a *maximin* optimized Latin Hypercube Sampling (LHS) – as described by Arora [17] – and parametrized within ANSYS Composites Preppost (ACP) and Ansys Fluent (for performing computational fluid dynamic – CFD – analyses). Parametrization goes according to the estimated number of plies and its material for the layup (ACP), and the wind speed and generator rotation (CFD). The simulations are conducted parametrically in reciprocal fluid structure interaction (2-way FSI). As for the simulation setup, CFD employs k-ω SST turbulence model with tetrahedral elements (a requirement for the FSI dynamic mesh), though prismatic elements are used in the far field for faster convergence and numerical stability. Structural analysis is conducted with SHELL281 structural elements and is considered elastic-linear, according to the CLT implemented by ACP, which computes the [ABD] matrix (eq. (8)) for the blade's laminates. Blade rotation is also considered in the structural analysis for the Coriolis effect. Other configurations, such as time stepping, iterations, CFD Courant number, etc. are selected according to the system's performance evaluated in the preliminary analysis.

To increase computational performance, a High Power Computing (HPC) cluster is configured integrating eight workstation nodes and a head node with Windows Server 2019 in a virtual machine. The full model simulations are run through the configured HPC in the UTFPR FSI laboratory. DOE stratification is also implemented for parallel solving of multiple design points.

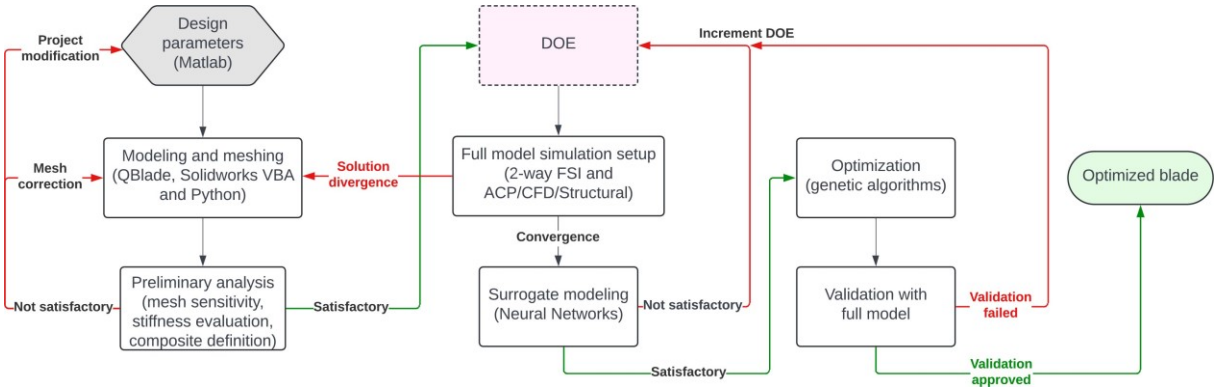

Figure 1. Workflow of the employed methodology

From the DOE and sampled data, an RBF ANN model is constructed and subsequently optimized by genetic algorithms, seeking maximum power output of the generator and constraining the maximum axial blade displacement to 5% of span length, thus reducing coning effects and avoiding tower collapse by blade strike. The optimization algorithm and the ANN are both configured by the author within Matlab (Gaussian process neural net) and programmed in **R** language (multilayered perceptron with Gaussian activation function neurons), assuring convergence of results.

$$\begin{aligned} \min_{\boldsymbol{x}} \quad & f(\boldsymbol{x}) = -\boldsymbol{P} = \omega.(-\boldsymbol{T}) \\ subject\ to \quad & g(\boldsymbol{x}) = max\ (\delta_x) \leq 5\%\ span \\ & -90 \leq x_j \leq +90 \end{aligned} \tag{11}$$

For the optimization procedure, as expressed in eq. (11), the torque, $\boldsymbol{T}$, is estimated from the surrogate, and used to compute the generator's output power, $\boldsymbol{P}$, from its rotation, ω. Since most optimization algorithms are better implemented in minimization problems, the formulation is to search for the minimum of the negative power. Genetic algorithms are then employed seeking the highest power output (or the minimum negative) as a function of the layup sequences (comprising $j = 6$ plies, discrete variables varying from -90 to +90° in 15°increments for manufacturability), while constraining the maximum axial displacement of the blade to 5% of span length.

4 Results

The parameters used to design the blade's geometry are presented in Tab. 1, both constructive and operational. During the preliminary analysis, a number of three plies are defined using Epoxy-Carbon unidirectional (UD) fibers, whose orthogonal properties are also presented in Tab. 1. These preferences are selected

due to the restricted blade's inner spacing, which allows only for a reduced number of plies. Its lack of volume is compensated by the selection of higher strength material, hence UD Epoxy-Carbon. Cheaper material such as Epoxy-Glass UD is also evaluated, however it yields unacceptable axial displacements and lower torque, hence it is not considered as an attractive solution. By utilizing Epoxy-Carbon UD, no samples presented maximum axial displacement greater than 5% span length. Therefore, no constraining is actually necessary, though it is implemented in the optimization algorithms nonetheless.

Table 1. Parameters used for the blade design

Parameter	Value	Comment
Power (theoretical)	660 W	Regarding the capacity of the generator's rotor
Wind nominal velocity	8 m/s	Rated speed of free current
Air density	1.184 kg/m³	Stipulated according to pressure and temperature (97 kPa and 16 °C)
Blade tip velocity ratio	8	Blade tip tangential velocity and wind speed ratio
Rotor-hub diameter ratio	0.10	Hub and rotor diameters ratio
Number of blades	3	Number of blades used in the generator
Lift coefficient	1.38	Defined according to the airfoil (NACA 4412)
Drag coefficient	0.0572	Defined according to the airfoil (NACA 4412)
Maximum angle of attack	14°	Stipulated according to the *expected* stall angle
Electromechanical efficiency	0.90	Efficiency in the electromechanical conversion of the generator
Number of elements (BEMT)	30	Number of elements along the blade span length
Young's modulus in direction 1	121 GPa	Selected composite ply material's E1
Young's modulus in direction 2	86 GPa	Selected composite ply material's E2
Shear modulus	4.7 GPa	Selected composite ply material's G12
Composite ply thickness	0.80 mm	Ply thickness for each lamina in the composite

Fifty-four sampling points are generated by LHS and simulated for the overload velocity of 16 m/s. The ply angles can vary from -90 to +90° in 15° increments – yielding a total of 13^6 (near 5 mi) possible layups – and the reference frame is a generator whose fibers all follow the span direction (i.e., zero-degree orientation). Figure 2 presents the blade geometry used for meshing. The hub is representative and its large dimensions and lower curvatures aims to lessen turbulence effects near the blade root.

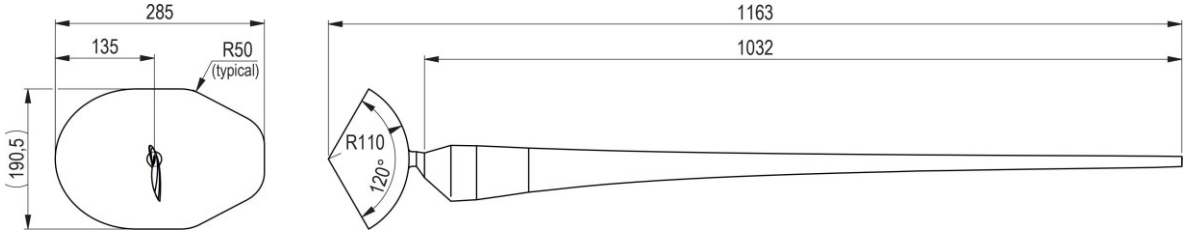

Figure 2. Blade geometry (dimensions in mm)

The genetic algorithm routine is employed restricting the inputs for discrete variables (15° increments). The surrogate is optimized with the sequences $[30 / 15 / 45]_U$ or $[30 / 15 / 60]_U$ for the upper surface (U), and $[0 / 15 / 45]_L$ for the lower surface (L). Table 2 presents a summary of the optimized results, including validation values.

Table 2. Genetic algorithm output summary

Matlab implementation (#1)	Value	**R** implementation (#2)	Value
Generations	105	Generations	88
Function evaluations (from surrogate)	6049	Function evaluations (from surrogate)	5210
Function value (torque)	3.2410 N.m	Function value (torque)	3.2315 N.m
Optimal sequence	$[30 / 15 / 45]_U \mid [0 / 15 / 45]_L$	Optimal sequence	$[30 / 15 / 60]_U \mid [0 / 15 / 45]_L$
Validated torque	3.2281 N.m	Validated torque	3.2815 N.m

Table 3 presents a summary of the main design points. According to the obtained values, the optimized laminate yields a 8.3% increased torque from the reference layup, and 2.8% from the highest DOE value, while

still maintaining a maximum axial displacement of less than 3% span length.

Table 3. Results summary for the main design points

Design point reference	Layup	Torque [N.m]	Max. axial displacement [mm]
Reference laminate	$[0 / 0 / 0]_U \mid [0 / 0 / 0]_L$	3.0296	20.478
Best DOE laminate	$[45 / 0 / 45]_U \mid [0 / 0 / 90]_L$	3.1934	26.088
Optimized laminate	$[30 / 15 / 60]_U \mid [0 / 15 / 45]_L$	3.2815	27.944

It is worth mentioning that one ANN is designed in Matlab and another in **R**, hence, the optimization procedures are also conducted with different algorithms, one in each platform. However, the obtained results in Matlab and **R** are similar, if not for the last ply in the upper surface.

5 Conclusions

A HAWT blade is designed through implementation of BEMT, and optimized to increase its power output in overload conditions. The composites ply materials are selected and the lamination sequences are parametrized and simulated in reciprocal fluid-structure interaction to evaluate the blade's performance in different layups.

Given the computational expenditure and time demand for simulation of the full model, a DOE is designed to construct a surrogate based on radial basis functions artificial neural networks, where inputs are the ply angles and the outputs are resultant torque and maximum axial displacement. The surrogate is optimized with genetic algorithms, seeking maximum torque while constraining axial displacement to attenuate the generator coning effect, and avoid tower collapse by blade strike. The obtained result is further validated with the full model, yielding acceptable error levels (less than 1.5%).

A torque increase of 8.3% is obtained, if compared to an unidirectional (span wise) configuration of the laminate (i.e., all plies at zero degree orientation). This is achieved while exponentially reducing the computation cost without sacrificing much accuracy, taking from hours for the full model to fraction of a second with the surrogate, and little deviation obtained comparing the responses of both models.

References

[1] Agência Nacional de Energia Elétrica. *Resolução Normativa n° 482/2012*. ANEEL, 2012.
[2] L. A. Hussni, "Avaliação do potencial eólico em ambiente urbano para aplicação de micro e minigeração distribuída: estudo de caso em edifício no centro da cidade de São Paulo". *Universidade de São Paulo*, 2021.
[3] L. Soriano, W. Yu and J. Rubio, "Modeling and Control of Wind Turbine". *Mathematical Problems in Engineering*, vol. 2013, n. 982597, 2013.
[4] A. D. Monte, M. R. Castelli and E. Benini, "Multi-objective structural optimization of a HAWT composite blade". *Composites Structures*, vol. 106, pp. 362-373, 2013.
[5] A. Mitra andA. Chakraborty, "Multi-objective optimization of composite airfoil fibre orientation under bending–torsion coupling for improved aerodynamic efficiency of horizontal axis wind turbine blade". *Journal of Wind Engineering and Industrial Aerodynamics*, vol. 221, n. 104881, 2022.
[6] Q. Zhang, W. Miao, Q. Liu, Z. Xu, C. Li, L. Chang and M. Yue, "Optimized design of wind turbine airfoil aerodynamic performance and structural strength based on surrogate model". *Ocean Engineering*, vol. 289, Part 2, n. 116279, 2023.
[7] L Vermeer, J. Sorensen and A. Crespo, "Wind Turbine Wake Aerodynamics". *Progress in Aerospace Sciences*, vol. 39, p. 467-510, 2003.
[8] T. Burton, D. Sharpe, N. Jenkins and E. Bossanyi, *Wind Energy Handbook*. Wiley, 2001.
[9] J. F. Manwell and J. G. McGowan, *Wind Energy Explained: Theory Design and Application*. 2. ed. Wiley, 2009.
[10] E. Hau, *Wind Turbines: Fundamentals, Technologies, Application, Economics*. 3. ed. Springer Berlin, 2013.
[11] M. Hansen, *Aerodynamics of Wind Turbines*. 2. ed. Routledge, 2008.
[12] R. Wilson and P. Lissaman, *Applied Aerodynamics of Wind Power Machines*. NTIS, 1974.
[13] J. Reddy, *Mechanics of Laminated Composite Plates and Shells: Theory and Analysis*. 2. ed. CRC Press, 2003.
[14] A. K. Kaw, *Mechanics of Composite Materials*. 2. ed. Taylor & Francis, 2006.
[15] A. B. Ryberg and R. D. Bäckryd, L. Nilsson, *Metamodel-Based Multidisciplinary Design Optimization for Automotive Applications*. 1st ed. Linköping University, 2012.
[16]A. I. J. Forrester, A. Sóbester and A. J. Keane, *Engineering Design via Surrogate Modeling: A Practical Guide*. 1st ed. Wiley. 2008.
[17] J. S. Arora, *Introduction to Optimum Design*. 2nd edition. University of Iowa, 2004.
[18] C. Tavares da Silva, "Método do Elemento de Pá Não Estacionário Aplicado ao Projeto de Pás de Turbinas Eólicas de Eixo Horizontal". *Doctorate thesis*. Instituto Tecnológico de Aeronáutica, 2011.